Dynamics of Water near a Protein Surface

Sarika M. Bhattacharyya, Zhen-Gang Wang,* and Ahmed H. Zewail*

Laboratory for Molecular Sciences and Division of Chemistry and Chemical Engineering, California Institute of Technology, Pasadena, California 91125

Received: July 31, 2003

In this paper, we develop a model for the dynamics of water near a protein surface and compare with experimental results obtained with femtosecond resolution. The model consists of a layer of bound and free water molecules at the surface of the protein in dynamic equilibrium with each other, coupled to bulk water away from the protein surface. A previous model (Pal et al. *J. Phys. Chem. B* **2002**, *106*, 12376) considered the exchange in the layer without the coupling to the bulk. We find that water dynamics at the protein surface are described by two time scales, a fast, bulklike time scale, and a slower one more than 1 order of magnitude longer. The slow time scale, as in the previous model, is shown to be inversely proportional to the bound-to-free water conversion rate, k_2, but with a significant dependence on the free-to-bound conversion rate k_1, the diffusion of the free water molecules, and the thickness of the layer. This effect, identified as the *feedback mechanism*, is found to depend on the degree of orientation of the bound water molecules at the surface. The weight of the contribution of the slow component to the overall relaxation dynamics is shown to be inversely proportional to the slow decay time. For a heterogeneous surface with spatially varying k_2, the water dynamics in a probe region covering several sites is described by the cumulated effects from these water molecules, with the slow dynamics given by a sum of exponentials, with contributions inversely proportional to their respective decay times. To a very good degree, we find that this exponential behavior can be *fitted* to a single exponential; however, the *apparent* time scale does not represent that of any particular site. These conclusions are in good agreement with experimental results and provide important insight to the observed dynamical behavior.

1. Introduction

Water plays a crucial role in determining the structure, dynamics, and function of proteins and other biological macromolecules. Although the dynamics of water in bulk has been extensively studied, its dynamics near a protein surface is still not fully understood. The dynamics and other properties of water near the surface is known to be quite different from those in the bulk, and this distinction has been elucidated experimentally using dielectric relaxation, NMR, and solvation dynamics methods (see refs 1−4 and references therein). Molecular dynamics simulations of proteins have also shown that water dynamics near the surface is indeed quite different from the bulk (see refs 5 and 6 and references therein).

Different categories of water behavior can be characterized depending on their residence times. One type is that strongly bound to (in) the protein, which can be identified crystallographically and play an important role in stabilizing the native structure. The residence time of these water molecules are usually in the range of 10^{-9} to 10^{-3} s. The other type of water is more dynamic (shorter residence times) and is of interfacial nature. The third type of water is in the vicinity of the protein surface but not directly interacting with the protein and behaves mostly like bulk water. Our main interest in this work is in the dynamics of hydration in the femtosecond−picosecond range to elucidate the nature of water at the interface with protein surfaces.

* Corresponding authors. E-mail: zgw@cheme.caltech.edu, zewail@caltech.edu.

In this laboratory we have been concerned with studies of hydration dynamics of proteins and DNA on the femtosecond−picosecond time scale, and in all the cases a "bimodal-like behavior" was observed: a femtosecond component that reflects a bulk-type behavior and a much slower picosecond component that is absent in bulk hydration.[1,7−9] The behavior was discussed[8] in terms of a "two-state" equilibrium between bound and free water in the layer. Such exchange was found by molecular dynamics simulations[6] and invoked in analytical models of micelle[10] and protein[1] hydration. However, the model did not consider the water dynamics beyond the surface layer and the dynamic coupling between the layer and bulk water. Moreover, it did not take into account the anisotropy in the water orientation near the protein surface.

Here, we present a model that takes into account these and other additional effects, and we compare our prediction with the experimental results. In our formulation of the model, using analytical expressions and numerical solutions, we consider the case where there is no restriction on the bound water orientation and also the case where all the bound waters have a unique direction.

2. The Model and Results

2.1. The Model. As in previous studies,[1,6,10] we assume that at the protein surface, water can exist in two states, bound and free, and that these two states are in dynamic equilibrium. The bound water is immobilized by the protein surface and thus cannot rotate or translate. The free water essentially behaves as

10.1021/jp030943t CCC: $25.00
Published on Web 11/01/2003

bulk water (and indeed these two terms will be used synonymously in this article) although their rotation and translation diffusion are generally modified due to their interaction with the protein. This surface layer of bound and free water is coupled to the bulk water outside the layer; this is a key feature neglected in previous studies. In addition, we allow the possibility of the bound water having a preferred orientation due to its interaction with the protein.

The protein surface is modeled as an infinite wall in the $x-y$ plane. This is clearly an approximation; however, the length scale of interest in this work is on the order of the radius of water (2.8 Å), which is much less than the radius of a typical protein (ca. 20 Å) and hence the protein surface can be considered to be locally flat.

We take a hydrodynamic approach wherein the water dynamics in the surface layer is described by a reaction diffusion equation and the bulk water dynamics is described by a simple diffusion equation. In this approach, the interactions are not considered explicitly but are understood to be reflected in the transport and rate parameters of the model. We comment here that, a priori, it is not clear that a hydrodynamic approach, which describes long wavelength, long time scale phenomena, is valid for the time and length scales we consider. Nevertheless, we adopt such an approach in this work on the basis of three considerations. First, a hydrodynamic approach allows us to focus on the effects of the bound and free water exchange and its coupling to bulk water dynamics in a simple and transparent way unencumbered by complicated details in the interaction potentials. Second, experimental results are often presented and explained using hydrodynamic concepts.[11] Finally, we are encouraged by the general success the hydrodynamic approaches have had in describing molecular phenomena. For example, it has been shown that the Stokes−Einstein relation between diffusion coefficients and viscosity holds down to molecular diameters.[12]

We describe the water dynamics by the time evolution of the orientation density of the free and bound water $\rho_f(r,\Omega,t)$ and $\rho_b(r,\Omega,t)$, respectively, which are defined as the probability density at position r, with orientation Ω, at time t, for the respective species. Thus, the time evolution for the free water density is given by

$$\frac{\partial}{\partial t}\rho_f(r,\Omega,t) = D\nabla^2\rho_f(r,\Omega,t) + D_R\nabla^2_\Omega\rho_f(r,\Omega\ t) - [\rho_f(r,\Omega,t)\int d\Omega_1\ k_1(\Omega,\Omega_1) - \int d\Omega_1\ \rho_b(r,\Omega_1,t)\ k_2(\Omega_1,\Omega)]h(z_L - z) \quad (1)$$

and that for the bound water by

$$\frac{\partial}{\partial t}\rho_b(r,\Omega,t) = -\ \rho_b(r,\Omega,t)\int d\Omega_1\ k_2(\Omega,\Omega_1) + \int d\Omega_1\ \rho_f(r,\Omega_1,t)\ k_1(\Omega_1,\Omega) \qquad \text{at} \qquad 0 < z < z_L \quad (2)$$

The first two terms on the right-hand-side of eq 1 describe the change in ρ_f due to translational and rotational diffusion, respectively. These terms are present in the entire semi-infinite space ($0 < z < \infty$). The third term represents the loss of free water due to a free-to-bound conversion where $k_1(\Omega,\Omega_1)$ is the transition rate from free water with orientation Ω to bound water with orientation Ω_1. The last term accounts for the creation of free water from bound water, where $k_2(\Omega,\Omega_1)$ similarly is the transition rate, from bound water with orientation Ω_1 to free water with orientation Ω.

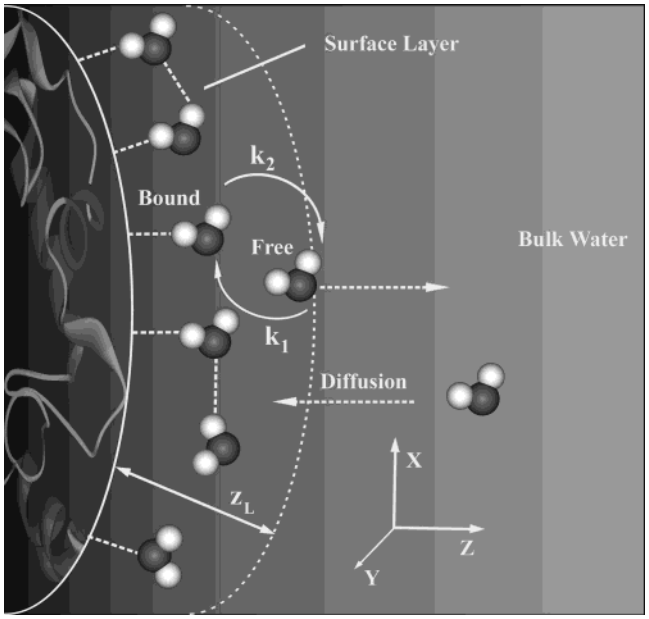

Figure 1. Schematic representation of the model. In the layer adjacent to the protein surface there are bound water molecules, hydrogen bonded to the protein surface (shown by dashed lines). There are also free water molecules that are not directly hydrogen bonded to the protein. There is a dynamic exchange between the free and the bound water inside the layer (shown by the solid curved arrows). The free water inside the layer can diffuse out to the bulk and some bulk water molecules can diffuse into the surface layer (shown by dashed arrows).

Because the bound water is assumed to exist only in the surface layer, these last two terms are only defined in this layer, which is taken into account by the presence of the Heaviside step function $h(z_L-z)$, where z_L is the width of the surface layer. In the case of bound water, because it cannot translate or rotate by itself, its density can only change because of transition between bound and free water; all terms in eq 2 are defined in the surface layer. Thus eq 1 couples the free water dynamics inside and outside the layer, and the free water dynamics inside the layer is coupled to the bound water dynamics through eq 2. The two equations together (eqs 1 and 2), introduce a coupling between the water in the surface layer and the bulk water outside this layer. A schematic representation of the model is given in Figure 1.

In eqs 1 and 2, the diffusion coefficients D and D_R and the interconversion rates k_1 and k_2 are assumed to be independent of position. Although the position dependence of these parameters can be readily incorporated into the equations, the resulting equations are no longer amenable to analytical solution. Thus in the analytical studies, we will treat these quantities as position independent parameters. However, we will consider the position dependence of k_2 in a numerical solution and will also discuss briefly the effect of the position dependence of the diffusion coefficients on our analytical results.

In writing eqs 1 and 2, it is implicitly assumed that the binding energy of the water to the protein surface is sufficiently large so that the bound states can be considered an identifiable species. Thus it is assumed that the transition rate of bound-to-free water is much slower than the dynamics of bulk water.

Because the width of the surface layer is only about one molecular diameter, in the spirit of the hydrodynamic approach it is convenient to regard this layer as a surface of zero thickness and consider the coupling between the water inside the surface layer and the bulk water outside the layer in terms of boundary conditions to the pure bulk water dynamics. Mathematically,

this is achieved by transforming the Heaviside step function into a Dirac delta function through the limiting process $\lim_{z_L\to 0}(1/z_L)h(z_L-z) = \delta(z)$. Equation 1 thus becomes

$$\frac{\partial}{\partial t}\rho_f(r,\Omega,t) = D\nabla^2\rho_f(r,\Omega,t) + D_R\nabla_\Omega{}^2\rho_f(r,\Omega,t) - [\rho_f(r,\Omega,t)\int d\Omega_1\, k_1'(\Omega,\Omega_1) - \int d\Omega_1\, \rho_b(r,\Omega_1,t)\, k_2'(\Omega_1,\Omega)]\delta(z) \quad (3)$$

where $k_1' \equiv k_1 z_L$ and $k_2' \equiv k_2 z_L$ are understood to remain finite. Equation 2 is now defined only at $z = 0$.

Equation 3 is equivalent to a bulk equation of motion plus a boundary condition, with the dynamics of the bulk water given by

$$\frac{\partial}{\partial t}\rho_f(r,\Omega,t) = D\nabla^2\rho_f(r,\Omega,t) + D_R\nabla_\Omega{}^2\rho_f(r,\Omega,t) \quad (4)$$

and the boundary condition given by

$$D\nabla_z\rho_f(r,\Omega,t) = \rho_f(r,\Omega,t)\int d\Omega_1\, k_1'(\Omega,\Omega_1) - \int d\Omega_1\, \rho_b(r,\Omega_1,t)\, k_2'(\Omega_1,\Omega) \quad \text{at} \quad z = 0 \quad (5)$$

The full dynamics is then described by eq 4, with boundary conditions given by eqs 5 and 2. As mentioned earlier, the boundary conditions give rise to the coupling between the surface layer and bulk water dynamics.

The free water in our model can assume all possible orientations. On the other hand the distribution of the bound water orientation can be quite site specific. The orientation of the bound water can be rigid or flexible, depending primarily on the number of hydrogen bonds it makes with the protein surface. For example a site where water makes one hydrogen bond with the protein has a larger orientational flexibility compared to the one that makes more hydrogen bonds. The water molecule that makes a large number of hydrogen bonds to the protein surface is highly rigid and its orientation will be fixed at a particular angle. To understand the effect of this orientational rigidity, we will consider two idealized limiting cases.

2.1.1. Case 1: Isotropic Bound Water Orientation. Here we assume that the bound water can exist in all possible orientations with equal probability. This means that free $\rightleftharpoons$ bound transitions can take place in all possible orientations. We assume that the transitions are independent of the angle of the free or bound water. We further assume that the orientation of the water molecule is preserved during the transitions. Thus the transition rate matrix can be written as

$$k_1(\Omega,\Omega_1) = k_1\delta(\Omega-\Omega_1)$$
$$k_2(\Omega,\Omega_1) = k_2\delta(\Omega-\Omega_1) \quad (6)$$

2.1.2. Case 2: A Single, Preferred Bound Water Orientation. Here we assume that the bound waters can reside only in one specific orientation, Ω_b. Thus the orientation dependence of the bound water density becomes a delta function, peaked at Ω_b,

$$\rho_b(r,\Omega,t) = \rho_b(r,\Omega_b,t)\,\delta(\Omega-\Omega_b) \quad (7)$$

Assuming as in case 1 that orientation is preserved during the transition, this means that the free-to-bound water transition can happen only at the specific orientation Ω_b and that the free water molecules created from bound water will have the instantaneous orientation of the bound water. The transition rates are now given by

$$k_1(\Omega,\Omega_1) = k_1\delta(\Omega-\Omega_1)\,\delta(\Omega_1-\Omega_b)$$
$$k_2(\Omega,\Omega_1) = k_2\delta(\Omega-\Omega_1) \quad (8)$$

The main body of this paper will focus on case 1, as this case is simpler yet captures most of the important effects we wish to highlight in this work. New effects due to fixed bound water orientation will be briefly discussed in section 2.4.

2.2. Choice of Parameters. Before we deal with specific cases, we briefly discuss the choice of the parameters in the model. Usually it is considered that the transition rates or the residence times of the free and bound waters are governed by the water−water and protein−water hydrogen bond energies.[1,10,13] The effect of electrostatic polarization from the protein is hidden in the strength of binding. In the bulk, water is extensively hydrogen bonded with an average of 2−3 hydrogen bonds per molecule.[14,15] Molecular dynamics simulations and other studies indicate that the fast dynamics in bulk water is due to a cooperative mechanism where energy is rapidly redistributed among nearby molecules as local defects in a hydrogen-bonded network.[16−18] The orientational relaxation time of bulk water has been measured to be 2.6 ps.[16]

In this study, we use the transition rates k_1 and k_2 taken to represent results of experiments in bulk water and in protein hydration. We take $k_1 = 0.1$ ps^{-1} and we use a range of k_2 values. We have varied the k_2 values to study the effect of the bound-to-free transition rate on the dynamics.

The translational and rotational diffusion of water near the protein surface is known to be slower than that in the bulk.[5] This effect can be taken into account in our model. However, to highlight the effect of the bound water on the dynamics we use the bulk translational and rotational coefficients. Thus, the rotational diffusion coefficient $D_R = 2.2 \times 10^{11}$ s^{-1} [5,19] and the translational diffusion coefficient $D = 2.3 \times 10^{-5}$ cm^2 s^{-1};[20] note that the experimental rotational relaxation time is 2.6 ps,[16] which gives $D_R = 1.9 \times 10^{11}$ s^{-1}, close enough to the deduced value in refs 19 and 20.

2.3. Case 1: Isotropic Orientation of Bound Water. In this subsection we consider the case where the bound water molecules can exist in all possible orientations. Although this case is highly idealized, it allows us to highlight the effects of bound-to-free water transition on the water dynamics within and outside the layer. In particular, it allows us to see clearly the origin of the slow dynamics through an analysis of the solution. We first address the case of uniform bound-to-free water transition rate by analytically solving the dynamic equations. We will then examine the consequence of site heterogeneity by solving the equations numerically to investigate the origin of the apparent single-exponential behavior observed in experiments on heterogeneous surface water.

With the transition rates given by eq 6, eq 2 reduces to

$$\frac{\partial}{\partial t}\rho_b(r,\Omega,t) = -\rho_b(r,\Omega,t)k_2 + \rho_f(r,\Omega,t)k_1 \quad \text{at} \quad z = 0 \quad (9)$$

and in a similar way the boundary condition, eq 5, reduces to

$$D\nabla_z\rho_f(r,\Omega,t) = k_1'\rho_f(r,\Omega,t) - k_2'\rho_b(r,\Omega,t) \quad \text{at} \quad z = 0 \quad (10)$$

Instead of solving for the full probability distributions $\rho_x(r,\Omega,t)$ ($x = f, b$), which involve both the spatial and orientation variables, it is more convenient to solve for the coefficients a_{lm}^x, defined through a spherical harmonics expansion of the

probability distributions $\rho_x(r,\Omega,t)$,

$$\rho_x(r,\Omega,t) = \Sigma a^x_{lm}(r,t)\, Y_{lm}(\Omega) \quad (11)$$

where $Y_{lm}(\Omega)$ are the spherical harmonics of rank l and projection m ($m = -l, -l+1, ..., l-1, l$). The lowest order coefficient a_{00} corresponds to the isotropic part of the density, whereas the coefficients a_{1m} represent the different components of the water dipole moment along the three orthogonal directions: $m = 0$ corresponding to the longitudinal component (defined, for example, by the dipolar orientation of the probe molecule) and $m = -1, +1$ to the two transverse components. For the case of isotropic distribution of free and bound water, the dynamics of the transverse and longitudinal components are identical. Furthermore, their dynamics are decoupled from each other and also from that of the isotropic density. Henceforth we consider only the longitudinal component, a_{10}, because this is the component whose dynamics is primarily probed in solvation dynamics experiments.[1,7−9] In the case of isotropic orientation, the choice of the longitudinal direction is immaterial. However, to be specific and for comparison with the case of preferred bound water orientation to be discussed later, we set the longitudinal direction to be the z direction.

The equations for a^f_{10} and a^b_{10}, which are obtained by substituting the spherical harmonics expansion (eq 11) into eqs 4, 9, and 10, can be further simplified by a Laplace−Fourier transform, resulting, after some rearrangements, in the following expressions,

$$\nabla_z^2 a^f_{10}(z,q,s) - \frac{1}{L^2} a^f_{10}(z,q,s) = -\frac{1}{D} a^f_{10}(z,q,t=0) \quad (12)$$

$$\nabla_z a^f_{10}(z,q,s) = \alpha a^f_{10}(z,q,s) - \frac{k_2'}{D(s+k_2)} a^b_{10}(z,q,t=0) \quad \text{at} \quad z = 0 \quad (13)$$

and

$$a^b_{10}(z,q,s) = \frac{k_1}{s+k_2} a^f_{10}(z,q,s) + \frac{1}{s+k_2} a^b_{10}(z,q,t=0) \quad \text{at} \quad z = 0 \quad (14)$$

where s is the Laplace variable conjugate to time, q is the momentum variable conjugate to position in the $x-y$ plane, $L^2 = D/(2D_R + D_q^2 + s)$, and $\alpha = k_1' s/(D(k_2 + s))$.

Equation 12 can now be solved using the method of Green's function.[21] For the free water we obtain

$$a^f_{10}(z,q,s) = \frac{1}{D}\int_0^\infty dz'\, a^f_{10}(z',q,t=0)\, G_T(z,z',q,s) + \frac{k_2'}{D(s+k_2)} a^b_{10}(z'=0,q,t=0)\, G_T(z,z'=0,q,s) \quad (15)$$

and for the bound water,

$$a^b_{10}(z,q,s) = \frac{k_1}{D(s+k_2)}\int_0^\infty dz'\, a^f_{10}(z',q,t=0)\, G_T(z,z',q,s) + \frac{a^b_{10}(z,q,t=0)}{s+k_2}\left[1 + \frac{k_2'}{D(s+k_2)} a^b_{10}(z'=0,q,t=0)\, G_T(z,z'=0,q,s)\right] \quad \text{at} \quad z = 0 \quad (16)$$

In eqs 15 and 16, $G_T(z,z',q,)$ is the Green's function in Laplace space,

$$G_T(z,z',q,s) = \frac{L}{2} e^{-|z-z'|/L} + \frac{L}{2} e^{-|z+z'|/L}\left(\frac{1-\alpha L}{1+\alpha L}\right) \quad (17)$$

The dynamics in the time domain is obtained by inverse Laplace transform of eqs 15 and 16.

Equations 15 and 16 describe the orientation relaxation of free and bound water at position z in response to the initial orientation of free and bound water molecules at position z'. Because the equilibrium distribution of both the bound and free water orientation is isotropic for the case considered here, the equilibrium value of a^f_{10} and a^b_{10} is zero. Thus, eqs 15 and 16 can be considered the linear response of the system to a small perturbation from equilibrium, which in turn can be related to the time correlation function at equilibrium by virtue of the fluctuation−dissipation theorem.[22] We comment here that the dynamic variables we are dealing with are not those that are directly measured in experiments on solvation dynamics, even though we will later use the conclusions drawn from our theoretical model to understand and predict the experimental results. In solvation dynamics the measured quantity is the decay of the solvation energy, which involves the dynamic structure factor of the solvent at all wavenumbers as well as the dynamic and structural information of the probe molecule.[23] Here we study the intrinsic dynamics of the solvent itself (albeit using a hydrodynamic description) without explicit reference to a probe. (The only information about the probe molecule that will be used is its size when we choose a value of the wavenumber q.) Insofar as the underlying dynamics of the solvent remains the same, the dynamic behavior predicted by our model can be related to the observed behavior in solvation dynamics.

In what follows, we present the key predictions for the isotropic case using eqs 15 and 16.

2.3.1. Time Scales of Water Dynamics at and Away from the Protein Surface. The full dynamic behavior of the system is described by eqs 15 and 16. However, these equations cannot be inverse Laplace transformed analytically, except in some asymptotic limits. We thus start with a presentation of the results obtained from numerically inverse Laplace transforming these equations.

Equations 15 and 16 suggest that water dynamics can be studied by perturbing at time $t = 0$ either the orientation of the free water molecules or that of the bound water molecules on the surface. We first consider the response of the system to initially oriented free water molecules. As will be argued below, the most significant contribution of water dynamics arises from the response of the water molecules on the surface to a perturbation on the surface. We will thus limit our considerations to this case.

In Figure 2, we show the dynamics of the free water molecules by monitoring the time evolution of a^f_{10} (dashed line in the figure) on the surface after an initial perturbation of the free water oriented in the z direction.[24] The bound-to-free transition rate for this calculation is chosen to be $k_2 = 0.096$ ps^{-1}. Because we will later make comparisons with results from solvation dynamics experiments, we choose the wavenumber q to correspond to the average diameter of the water and tryptophan probe, as it has been shown that the primary contribution in solvation dynamics of dipolar liquids comes from the first solvation shell.[23,25] Thus we set $q = 2\pi/1.5\sigma$, assuming an average probe-solvent diameter of 1.5σ, where σ is the diameter of water. The decay of a^f_{10}, shown with dashed line, actually involves two different time scales, and the long time dynamics is exponential with a slow time scale τ_{slow}. However, the presence of the slow component is hardly perceptible on

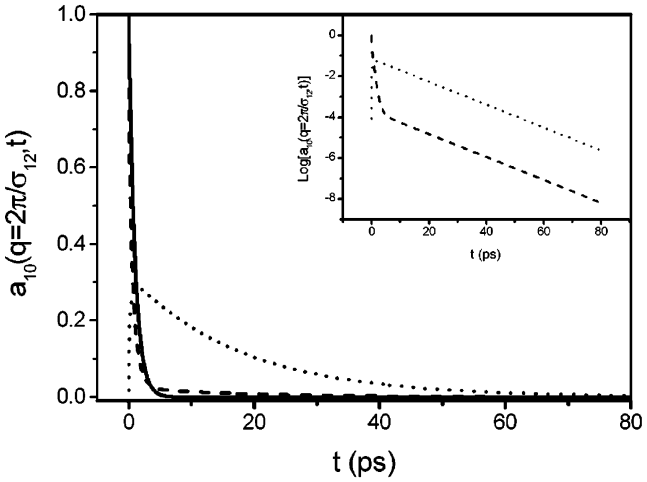

Figure 2. Dynamics of the longitudinal moment, a_{10}, of the free water in the surface water layer (at $z = 0$) plotted against reduced time for the bound-to-free conversion rate, $k_2 = 0.096$ ps^{-1}. The solid line represents the water dynamics at a nonbinding site. The dashed and the dotted lines represent the water dynamics at a binding site where initially there is a free and a bound water oriented in the preferred direction, respectively. Significant contribution to the slow component (τ_{slow}) comes from a site where initially there is a bound water oriented in a specific direction. In the inset we plot the ln a_{10} (at a binding site) against reduced time to show that in the long time at a binding, both cases have identical time scale.

the scale of the figure because its contribution is quite small. The slow component becomes evident on a semilog plot; see the inset in Figure 2.

We next study the free water dynamics on the surface by initially orienting the bound water in the preferred z direction by setting $a_{10}^{f}(z',q,t=0) = 0$ at all positions and $a_{10}^{b}(z'=0,q,t=0) = 1$ in eq 15. The result is shown in Figure 2 as a dotted line. In this case, because the free water orientation is unperturbed initially, $a_{10}^{f} = 0$ at $t = 0$. However, because bound water converts to free water as time evolves, the number of free water molecules in the preferred direction increases. It goes through a maximum and then decays exponentially with the same time scale, τ_{slow}, as seen more clearly on the semilog plot (dotted line). Thus, for both types of perturbation, the dynamics in the long time is exponential and the slow time scale, τ_{slow} is the same.

Thus far in describing our model, the protein surface ($x-y$ plane) is assumed to be homogeneous; hence bound water can exist on all the surface sites. In reality the protein surface has both hydrophilic and hydrophobic groups. On the surface along with the water binding sites there are also sites that do not bind any water molecule. At these positions the free $\rightleftharpoons$ bound transitions are absent. The water dynamics in that case will have only the fast bulklike dynamics, which is exponential and shown in Figure 2 by a solid line. If we compare the dashed and the solid lines, we find that at a binding site due to the effect of free $\rightleftharpoons$ bound transitions the fast dynamics is faster than the bulklike dynamics of a nonbinding site.

In principle, all three types of dynamics mentioned above will be present in the composite surface water dynamics. The dynamics thus can be obtained by adding the solid, dashed, and the dotted lines in Figure 2 weighted by the fraction of nonbinding and binding sites on the surface and among the binding sites by the fraction of free and bound water, respectively. Because the solid and the dashed lines are dominated by the fast dynamics and the dotted line by the slow dynamics, the fraction of free (in nonbinding and binding sites) and bound water determines the weight of the fast and the slow dynamics, respectively.

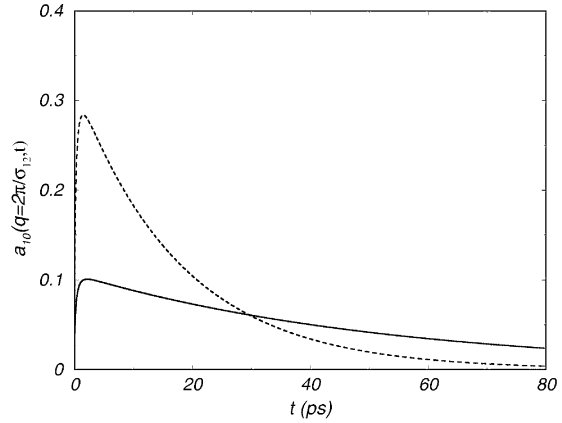

Figure 3. Dynamics of the longitudinal moment, a_{10}, of the free water in the surface water layer (at $z = 0$) plotted against reduced time for two different values of k_2. The solid line corresponds to $k_2 = 0.032$ ps^{-1} and the dashed line corresponds to $k_2 = 0.096$ ps^{-1}. Smaller k_2 value leads to a longer τ_{slow} but a smaller contribution of the longtime component.

It is evident that the primary contribution to slow dynamics comes from positions where initially a bound water is oriented. Because in our model bound waters exist only in the surface layer, there will be no significant contribution to the slow dynamics beyond this first layer. Henceforth, only the dynamic response in the surface layer will be considered.

2.3.2. Effects of Bound-to-Free Transition Rate on the Slow Dynamics. The lifetime of a bound water varies in different protein−water systems. Even in the same system, it can differ from site to site. To examine the effects of the bound water lifetime on the dynamics, we compare the dynamics of a_{10}^{f} of the free water in the surface layer at two different values of k_2, the bound-to-free water transition rate. Conclusions drawn from this study will also be used to understand the apparent single-exponential decay when site inhomogeneity is present. As demonstrated in the last subsection, the primary contribution to the slow dynamics is due to perturbation in the orientation of the bound water; we thus focus our consideration to this initial condition.

Figure 3 shows the behavior of a_{10}^{f} at the two k_2 values, $k_2 = 0.096$ ps^{-1} and $k_2 = 0.032$ ps^{-1}. Clearly, the smaller k_2 leads to longer τ_{slow}. This is in qualitative agreement with earlier theoretical work that predicted $\tau_{slow} \leq k_2^{-1}$, although we will show in the next subsection that our predicted τ_{slow} includes an additional term that reflects the combined effects of interconversion of free and bound water, the diffusion of free water and the width of the surface layer. The feature we wish to highlight in this subsection is the observation that a decrease in k_2 results in a decrease in the peak value of a_{10}^{f}. In fact, we find that when the diffusion coefficients and the free-to-bound transition rates are fixed, then the peak value is directly proportional to k_2. If we approximate the overall dynamics by a sum of two exponentials that represent respectively the fast and slow components (given respectively by the initial fast decay of the solid and the dashed curve and the slow decay of the dotted curve in Figure 2, weighted properly by the fraction of binding and nonbinding sites and among the binding sites by the fraction of free and bound water molecules near the probe), as is often done in the analysis of experimental data, then this result means that the percentage contribution of the slow component decreases with decreasing k_2. This effect can be understood physically by the argument that, in a system with

TABLE 1: Summary of the Experimental Results of Solvation Dynamic for Protein Monellin, Subtilisin Carlsberg (SC), and α-Chymotrypsin (CHT) at Two Different pHs[a]

system	position of the probe	τ_{fast} (ps)	% contribution of τ_{fast}	τ_{slow} (ps)	% contribution of τ_{slow}
SC	α-helix	0.8	61	38	39
monellin	*β*-sheet	1.3	46	16	54
α-chymotrypsin					
at pH 3.6	N-terminus	0.4	50	43	50
at pH 6.7	N-terminus	0.8	90	28	10

[a] For monellin and SC system, the solvation correlation function, $C(t)$, is fitted to a biexponential decay. The position of the probe in those systems, the fast and the slow time scales (τ_{fast} and τ_{slow}) and their contribution to the total dynamics are given. For the CHT, $C(t)$ can be fitted to three exponentials, two of which are due to the fast component. Here the slow time scale and its contribution to the total dynamics are given together with the average of the two fast components.

more rigid bound water, i.e., a smaller k_2 value, there are fewer (oriented) bound-to-free water transitions in a given time in the surface layer, which results in a smaller contribution of the more rigid bound water to the water dynamics.

These conclusions offer a possible explanation to the experimental findings by Pal et al.[7−9] In making the comparison, we emphasize again that the dynamic variable we consider in the model is not directly the relaxation of the solvation energy. However, for a static solute, if we choose the wave vector that corresponds to the dominant contribution to the solvation energy, then the time scales of the solvent dynamics (at that wave vector) along with the weight of the different time scales is expected to be reflected in the solvation energy correlation function.

The relevant experimental data are summarized in Table 1. In the first set of experiments, these authors studied the water dynamics near the monellin and subtilisin Carlsberg (SC) protein surfaces using intrinsic tryptophan (Trp) fluorophore as the probe. In the monellin case, the probe is near a hydrophobic *β*-sheet, whereas in the SC case, the probe is near a hydrophilic α-helix (refer to Table 1). Thus the water near the Trp in SC is expected to be more rigid (lower k_2 value). This explains the experimentally observed longer τ_{slow} in the SC system than in the Monellin system. The percentage contribution of the slow component is less for the SC than for Monellin, again in agreement with our theoretical prediction. Note that this is so even though the number of bound water molecules in the SC (α-helix) is expected to be larger, which by itself would have increased the contribution of the slow component. If the number of bound water molecules near the probe were the same for SC and monellin, we would see an even smaller contribution of the slow component in SC than in Monellin.

The second set of experiments studied the solvation dynamics at the α-chymotropsin surface at two different pH values. The slow time scale τ_{slow} is longer for the lower pH (3.6) and also the percentage contribution of the slow time scale is larger; see Table 1. According to our theory this is possible only if there is a larger number of bound water at lower pH. Note that in this study, the probe (ANS) is near an amino group. At lower pH, due to the protonation of the amino group, there are more protons on the protein surface to form hydrogen bonds with the water molecules. Apparently this effect dominates over the increased lifetime of the bound water, which by itself would have decreased the contribution of the slow component.

2.3.3. Analysis of the Time Scales and the Origin of τ_{slow}. In this subsection, we present an analysis of the time scales of the dynamics with an emphasis on the slow time scale, τ_{slow}. Due to the complicated form of the dynamics in the Laplace space (given by eqs 15 and 16), it is difficult to obtain an analytical expression for the water dynamics in the entire time domain. However, it is possible to perform an asymptotic analysis and obtain analytical expressions for the fast and the slow time scales, τ_{fast} and τ_{slow} respectively.

As shown in Figure 2, the fast dynamics of a binding site is nonexponential and decays faster than the fast dynamics of a nonbinding site. In the absence of a binding site the water dynamics is given by eq 15, with k_1 and k_2 set to zero. An asymptotic analysis reveals that the leading behavior of the water dynamics in this case is an exponential decay with a time constant

$$\tau_{fast} = (2D_R + Dq^2)^{-1} \tag{18}$$

which is identical in form to that given by previous theory.[1]. However, due to the breaking of the translational symmetry of the system by the presence of the protein surface in our model, the wavenumber q in our expression is conjugate only to the two-dimensional $x-y$ plane whereas the bulklike dynamics reported earlier[1] involves a three-dimensional wavenumber.

The slow time scale is found to arise from the combination of the first and second term in eq 17, namely, the function $1/(L^{-1} + \alpha)$. This term reflects the coupling between the surface layer and the bulk water. The slow time scale can be identified by performing an asymptotic analysis for the Laplace variable $s < \tau_{fast}^{-1}$. The analysis leads to the following expression for τ_{slow},

$$\tau_{slow} = \frac{1}{k_2} + \frac{k_1'}{Dk_2\left(\frac{2D_R + Dq^2}{D}\right)^{1/2}} \tag{19}$$

Using eq 18 for the fast time scale, and recalling that $k_1' \equiv k_1 z_L$, we can write the above equation as

$$\tau_{slow} = \frac{1}{k_2}\left[1 + (k_1\tau_{fast})^{1/2}\frac{z_L}{\lambda}\right] \tag{20}$$

where $\lambda \equiv (D/k_1)^{1/2}$; it is the length scale a molecule diffuses within the reaction time k_1^{-1}. The inverse k_2 dependence of τ_{slow} is expected and has also been predicted by previous theory.[1] The presence of the additional term is one of the key predictions of our study.

We now discuss the physical content of this additional term based on eq 20. Once a bound water becomes a free water, it can undergo a translational and rotational diffusion and randomize its orientation, or it can bind back to the protein surface. Thus there is a competition between the free-to-bound transition rate, k_1, and the randomization rate of a free water, τ_{fast}^{-1}. Noting that k_1^{-1} is the time scale for the free-to-bound transition, we may interpret $\tau_{fast}k_1$ as the probability (unnormalized) that a free water molecule has not relaxed its orientation during the time of a free-to-bound transition. Similarly, the ratio z_L/λ can be interpreted as the fraction of free water molecules that remain in the surface layer within the time scale of the free-to-bound transition. These two terms, in combination with the $1/k_2$ factor, can thus be understood to represent the probability that a free water molecule created by a bound-to-free transition, remains in the surface layer and has not relaxed its orientation, when the reverse free-to-bound transition occurs. Such a free-to-bound transition in the original orientation of the bound water obviously slows down the relaxation of the water orientation by feeding

TABLE 2: Summary of the Experimental Solvation Dynamic Results in Native and Denatured Monellin[a]

system	position of the probe	τ_{fast} (ps)	% contribution of τ_{fast}	τ_{slow} (ps)	% contribution of τ_{slow}
monellin					
native	β-sheet	1.3	46	16	54
denatured		3.5	72	56	28

probe	solution	τ_1^{bulk}	% contribution of τ_1^{bulk}	τ_2^{bulk}	% contribution of τ_2^{bulk}
Trp	0 M GdnHCl	0.18	20	1.1	80
Trp	6 M GdnHCl	0.57	28	4.4	72

[a] The solvation correlation function, $C(t)$, is fitted to a biexponential decay. The fast and the slow time scales (τ_{fast} and τ_{slow}) and their contribution to the total dynamics are given. The results of solvation dynamics study of Trp in bulk water and in 6 M GdnHCl solution are also given. $C(t)$ has a fast part, τ_1^{bulk}, and slow part, τ_2^{bulk}.

the bound water with molecules in the original orientation. We thus call this mechanism a *feedback mechanism*.

The contribution of the second term in eq 20 is significant. If we use the values for k_1, D, D_R, z_L, and q mentioned in the earlier subsections, we find $\tau_{slow} = 1.7/k_2$. Thus, our predicted τ_{slow} is 1.7 times longer than that predicted by previous theory.[1] If the free-to-bound transition is faster, or if the diffusion coefficient near the surface is smaller than the bulk value, as suggested in simulation studies,[5] the correction term due to the feedback mechanism will be even more significant.

Our result for the slow time scale can be used to compare with the solvation dynamics results by Pal et al. in a salt-denatured protein system[1] (refer to Table 2). In addition, we infer from the analysis that the addition of salt increases the lifetime of the bound water on the protein surface.

Salt is known to have significant effects on water dynamics. Computer simulation[26] has shown that the presence of salt weakens the water−water hydrogen bond and thus leads to a decrease in the lifetime of the hydrogen bond. The simulation has also shown that the addition of salt reduces the diffusion coefficients for both translation and rotation as a result of the increased friction due to the ion presence. This latter effect is in accord with the Onsager−Fuoss theory.[27] The relevant data from the computer simulation in ref 26 can be summarized as follows: For 0 M NaCl solution, $D = 2.75$ and $\tau_{HB} = 0.54$ ps; for 3.35 M NaCl solution, $D = 1.70$ and $\tau_{HB} = 0.50$ ps. τ_{HB} denotes hydrogen bond lifetime and D is the diffusion coefficient, which is scaled by 10^{-5} cm^2 s^{-1}.

The slowing down of the diffusion coefficients leads to an increase in the fast time scale; see eq 18. This is indeed the case as demonstrated by an increase in both τ_{fast} in the denatured protein system and τ_{bulk} in bulk salt solution. From these time scales, we infer that the diffusion coefficients are reduced by a factor of 2.7 in the denatured protein system relative to the native condition. From the simulation results we find that with a reduction of the diffusion coefficients by a factor of 1.6, the lifetime of the hydrogen bond decreases by a factor of 1.08. Assuming a simple proportionality, with a reduction of the diffusion coefficients by a factor of 2.7 (as obtained from the experimental results), the lifetime of the hydrogen bond is expected to decrease by a factor of 1.8.

We interpret the latter as implying that k_1 is now 1.8 larger. These effects would lead to an increase of the slow time scale τ_{slow} by a factor of 2.5. Experimentally, a larger increase in τ_{slow} is obtained (3.5 times). To account for this increase, per our eq 19, the bound-to-free transition rate k_2 must decrease. A decrease in k_2 is indeed consistent with the decreased percentage weight of the slow component of the dynamics in the denatured case relative to the native condition. Thus our analysis suggests that the increase of the slow time scale in the denatured protein system is the result of a cumulative effect due to the increased free-to-bound transition rate, decreased diffusion coefficients, and also decreased bound-to-free transition rate.

The increase in the lifetime of the bound water due to the addition of salt can be rationalized using the cooperative mechanism for water dynamics alluded to in section 2.2.[2,17,18] According to this mechanism, the breaking of the water−protein hydrogen bond is due to a rapid energy redistribution among nearby molecules through the hydrogen-bond network. This cooperative mechanism is possible only when the bound water is well connected to the bulk water. Because it has been shown that the addition of salt leads to a disruption of the water−water hydrogen bond, it is reasonable to speculate that salt can similarly decrease the connectivity of the bound water and the water surrounding it, thus resulting in a longer lifetime of the protein−water hydrogen bond. Further studies will be necessary to confirm this speculation.

2.3.4. Heterogeneous Surfaces. Our analysis thus far assumes a single binding energy for all the bound water molecules in the surface layer. In reality, a protein surface is heterogeneous with a distribution of binding energies or the bound-to-free water transition rate, k_2. Because k_2 determines the slow time scale, a distribution of k_2 leads to a distribution of the slow time scales, whose superposition is generally expected to yield stretched exponential behavior. However, solvation dynamics studies on heterogeneous surfaces reported by Pal et al.[1,7−9] show that the long time behavior is well described by an exponential decay with a well-defined decay time.

To understand this observation, we have introduced a spatial inhomogeneity in k_2 in our model. This is done by introducing binding sites in the surface layer that are equally spaced in the $x-y$ direction but with a distribution of the k_2 value. The resulting equations are solved numerically by using a finite difference scheme.

Our numerical results show that for the long time dynamics, there is no interference between neighboring binding sites if the sites are separated by more than a water diameter away. This is not surprising because the time it takes for a water molecule to diffuse a distance of its diameter is 4 ps whereas orientational relaxation occurs on the time scale of 2.3 ps. Thus by the time a water molecule visits its neighboring site its orientational relaxation is all but complete.

The absence of interference between neighboring binding sites greatly simplifies the dynamics of water at a heterogeneous surface. Because we have shown that the weight of the slow component with a single type of binding site is inversely proportional to the slow decay time, the slow component of the dynamics due to several types of binding sites should be a sum of exponentials, each weighted by the inverse of its slow time scale. In Figure 4 we construct such a sum of eight exponentials with equally spaced time scales between 10 and 50 ps, $F_1(t) = \Sigma_i 1/\tau_i \exp(-t/\tau_i)$. This function can be well-fitted to a single exponential with a relaxation time $\tau = 17.5$ ps. For comparison, we show in the same figure the function $F_2(t) = \Sigma_i \exp(-t/\tau_i)$, which essentially exhibits a stretched exponential behavior. The reason for the observed single exponential behavior in the slow dynamics is the particular manner in which the dynamics associated with each site is weighted (i.e., inversely proportional to its decay time). Thus the experimentally observed slow time scale is an *apparent* one that approximates the

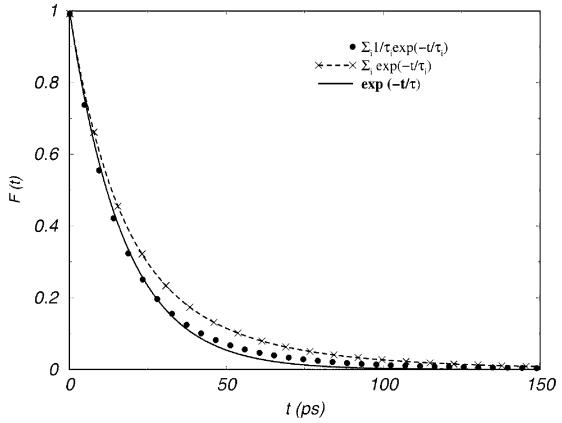

Figure 4. Apparent single-exponential relaxation in the water dynamics from a heterogeneous surface layer. The filled circles represent the function, $F_1(t) = \Sigma_i 1/\tau_i \exp(-t/\tau_i)$. The crosses connected by dashed line represent the function $F_2(t) = \Sigma_i \exp(-t/\tau_i)$. In both cases we have considered eight values of τ, equally spread between 10 and 50 ps. The solid line is an exponential fit for F_1, with time scale of 17.5 ps.

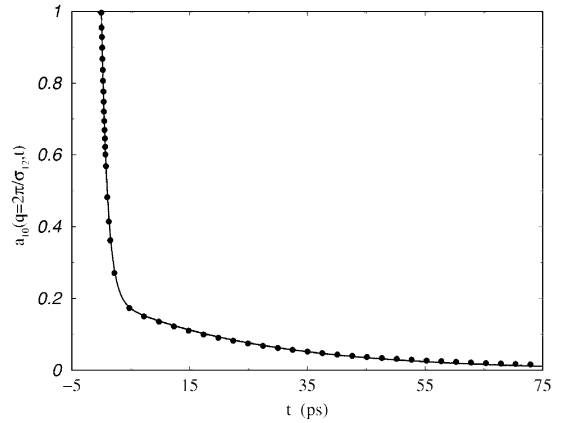

Figure 5. Composite water dynamics from a heterogeneous surface layer (solid circles) fitted to a biexponential function (solid line), where $\tau_{fast} = 1$ ps with 80% contribution and $\tau_{slow} = 26$ ps with 20% contribution. We have assumed that one-third of the sites do not bind any water molecule, and 80% of the binding sites remain occupied with bound water (the binding sites have different bound-to-free transition rates, $k_2 = 0.08$, 0.06, 0.04, 0.02 ps^{-1}).

cumulative effect of the different participating bound sites with their proper weight but does not correspond to the decay time of a particular site.

Next we show that the total water dynamics from a heterogeneous surface layer can be fitted to a biexponential as is often done in the analysis of experimental results.[1,7,8,9] The surface layer water dynamics is inherently heterogeneous and contains contribution from free water at nonbinding sites and free water at binding sites where the binding sites have different bound-to-free transition rates, k_2. As an example, assuming that one-third of the sites do not bind water molecules, and 80% of the binding sites remain occupied with bound water,[5] we obtain a composite water dynamics shown as solid circles in Figure 5. The data can be fitted to a biexponential (given by the solid line) where $\tau_{fast} = 1$ ps with 80% contribution and $\tau_{slow} = 26$ ps with 20% contribution. Note that the fast dynamics is a composite of the dynamics at nonbinding sites (solid curve in Figure 2) and binding sites (dashes and dotted curves in Figure 2). The more contribution to the fast dynamics we have from the binding sites occupied with free water, the shorter will be the apparent fast decay time.

2.4. Case 2: Effects of Preferred Bound Water Orientation. In the previous section we have considered the orientation of the bound waters to be isotropic. This simplified assumption allows us to focus on the dominant effects due to the bound-to-free water transition and due to the dynamic coupling between the surface layer and the bulk. In this section, we consider the more realistic situation where the bound waters may be preferentially oriented with respect to the protein surface. Because we have just shown that different binding sites on the protein surface contribute to the water dynamics essentially independently when the sites are more than a water diameter apart, it suffices to consider the case where all binding sites have the same preferred orientation.

In two special cases where the bound water orientation is either parallel or perpendicular to the surface, the equations can be solved analytically. For other orientation angles, we have solved the equations numerically.

We find that the main conclusions drawn for the case of isotropic bound water orientation remain valid. These are that the presence of the slow dynamics is significant only in the surface layer, that the free-to-bound transition and the coupling to the bulk introduces a feedback mechanism with an appreciable contribution to the slow decay time, that the percentage contribution to the slow dynamics is inversely proportional to the lifetime of the bound water, and that binding sites more than a water diameter apart independently contribute to the water dynamics. However, having a preferred orientation with respect to the surface considerably increases the complexity of the analysis. Instead of reproducing the details of the analysis, here we merely point out a couple of new effects that are not present in the isotropic case; an outline of the analysis is presented in the Appendix.

Whereas in the case of isotropic bound water orientation the longitudinal and transverse dynamics are identical and are decoupled from each other as well as from the isotropic part of the water density, once there is a preferred orientation, these different components of the dynamics become coupled. The slow time scale cannot be attributed to each individual component, which reflects the dynamic coupling of these components. Following a similar asymptotic analysis as in the case of isotropic bound water, we obtain the following expression for the slow time scale in the present case,

$$\tau_{slow} = \frac{1}{k_2} + \frac{3k_1'}{4\pi D k_2 \left(\frac{2D_R + Dq^2}{D}\right)^{1/2}} + \frac{k_1'}{4\pi D k_2 \left(\frac{Dq^2}{D}\right)^{1/2}} \quad (21)$$

Two points about this expression are noteworthy. First, the slow time scale is independent of the specific angle of the preferred orientation. This is so because the density of the free water is unaffected by the specific orientation of the bound water. Consequently, the number of free water molecules participating in the free-to-bound transition, and hence the feedback mechanism, is independent of the bound water orientation. Second, in comparison to eq 19, having a preferred orientation of the bound water reduces the effects of the feedback mechanism. Because the interconversion between bound and free water can take place at only one specific angle, the number of free water molecules that participate in the feedback mechanism decreases compared to the isotropic case.

Although the predicted slow time scale is independent of the bound water orientation and is identical for the transverse and longitudinal components of the dipole, the percentage contribution to the slow dynamics is generally different for the longitudinal and transverse components. The dynamics in any orientation that is parallel to the bound water orientation has

the maximum contribution to the slow dynamics whereas dynamics in the orthogonal orientation does not contribute at all. For example, if the bound water is oriented along the z direction (which is defined to be the longitudinal direction), then the longitudinal component of the moment has the maximum contribution, and the transverse components (in the $x-y$ direction) do not have any contribution to the slow dynamics. For an arbitrary angle of orientation of the bound water, however, both the longitudinal and transverse components of the dynamics will have the slow component present because the component parallel to the bound water orientation will involve a linear combination of the longitudinal and transverse components.

3. Conclusion

In this article we have presented a study of the water dynamics near a protein surface. Our model builds upon an earlier model that accounted for the interconversion between bound and free water at the protein surface but includes the coupling between the surface layer and the bulk. An explicit surface layer coupled to the bulk introduces spatial inhomogeneity in the direction perpendicular to the surface and also sets the necessary coordinate frame for defining the orientation of the water molecule; these are the two important physical features that were ignored in the previous model.

One of the key results of our study is the prediction that the slow time scale, τ_{slow}, is slower than the bound-to-free transition rate, k_2^{-1}, predicted by previous study.[1] The additional contribution, given by the second term in eq 19, arises from a feedback mechanism whereby a free water, partially relaxed or unrelaxed (through translational and rotational diffusion) from the orientation of a bound water from which it is created, is converted back to the bound state. Using reasonable estimates of the parameters, we find that the magnitude of this contribution is comparable to the inverse bound-to-free transition rate, k_2^{-1}. However, restricting the orientation of the bound water reduces the effects of the feedback mechanism due to the reduction in the number of water molecules that can make free-to-bound transition. The other important result is the finding that the percentage contribution of the slow component in the overall dynamics is inversely proportional to the slow lifetime of water molecules.

In addition, we find that bound waters at different binding sites on a heterogeneous protein surface contribute independently to the slow dynamics with no interference between different sites when they are separated by distances more than the size of a water molecule. Thus in a heterogeneous surface layer (as is probably the case for most protein-water systems), the slow part of the total water dynamics consists of a sum of exponentials associated with each site but weighted by a factor inversely proportional to the local slow decay time. The behavior of this composite function is found to be well fitted by an apparent single exponential, with an *apparent* decay time that does not reflect a particular site. Similarly, the fast component of the dynamics generally consists of contributions from free water at nonbinding and binding sites and the apparent fast time scale is intermediate between that associated with the bulk dynamics and that associated with the fast component of free water dynamics at the binding sites.

These predictions offer important new insights to the observations we have made in this laboratory on a number of protein−water systems using solvation dynamics with femtosecond resolution. In particular, the observed single exponential decay at long time in the solvation energy for heterogeneous protein surfaces, where stretched exponential is usually expected, can now be explained by the reasoning given in the preceding paragraph. The predicted inverse relationship between the slow time scale and the percentage contribution of the slow component of the dynamics is also qualitatively consistent with experimental results for monellin and subtilisin Carlsberg.[1,7,8] Furthermore, our predicted slow decay time scale suggests a possible explanation for the observed increase in the slow decay time of the denatured protein as compared to the native protein system.[9] In an earlier study the slow decay time was described in terms of polymer dynamics.[1] Here we have argued that addition of salt in the system shifts both the fast and the slow time scale to a longer time and also predicted that addition of salt increases the hydrogen bond lifetime of bound water.

Although our phenomenological, hydrodynamic model captures some important qualitative effects due to the interconversion between bound and free water at the protein surface and the coupling between dynamics in the surface layer and dynamics in the bulk, the actual water dynamics is likely to be considerably richer and more complex. For example, even at the same binding site, the bound-to-free transition rate may vary with time depending on the specific configuration of the local environment of the hydrogen bond network if the lifetime of the network is longer or comparable to the lifetime of the bound water. Thus the transition rate itself can become a dynamic property. We hope to address effects such as this in future work.

Acknowledgment. This work was supported by the National Science Foundation. We thank Dr. Samir K. Pal for stimulating discussion and help. S.M.B. thanks Prof O. Bruno, Dr. A. Kamal, and A. Mukherjee for helpful discussions.

Appendix

Here we present the key steps used to calculate the dynamics of the isotropic density and transverse and longitudinal components of the water dipole moment when the bound water is oriented in a preferred orientation (Case 2). For this case the bound water density and the transition rates are given by eqs 7 and 8, respectively. Replacing these expressions in eq 2 the bound water dynamics reduces to

$$\frac{\partial}{\partial t}\rho_b(r,\Omega_b,t) = -\rho_b(r,\Omega_b,t)k_2 + \rho_f(r,\Omega_b,t)k_1 \qquad \text{at} \qquad z = 0 \tag{22}$$

Although eq 22 looks similar to eq 9, in the latter, the transition between the bound and free water can happen at all possible orientations whereas in the former the transitions are restricted at a particular orientation.

Similarly, the boundary condition (eq 5), after taking a product with $Y_{lm}(\Omega)$ and integrating over Ω reduces to

$$D\nabla_z a_{lm}^{\,f}(r,t) = k_1'\rho_f(r,\Omega_b,t)\,Y_{lm}(\Omega_b) - k_2'\rho_b(r,\Omega_b,t)\,Y_{lm}(\Omega_b) \qquad \text{at} \quad z = 0 \tag{23}$$

The bound water dynamics (eq 22) and the boundary condition (eq 23) can be simplified by taking a Laplace−Fourier transform and after some rearrangements reduces to

$$\rho_b(z,q,\Omega_b,s) = \frac{k_1}{s+k_2}\rho_f(z,q,\Omega_b,s) + \frac{1}{s+k_2}\rho_b(z,q,\Omega_b,t{=}0) \qquad \text{at} \quad z = 0 \tag{24}$$

$$\nabla_z a_{lm}^{\,f}(z,q,s) = \alpha\rho_f(z,q,\Omega_b,s)\,Y_{lm}(\Omega_b) - \frac{k_2'}{D(s+k_2)}\rho_b(z,q,\Omega_b,t{=}0)\,Y_{lm}(\Omega_b) \qquad \text{at} \qquad z = 0 \tag{25}$$

where s is the Laplace frequency conjugate to time, q is the momentum variable conjugate to position in the $x-y$ plane, and $\alpha = k_1's/(D(k_2 + s))$.

In eq 25 when we expand the densities in the spherical harmonics (as given by eq 11), in the right-hand side we have contributions from all the spherical harmonic coefficients. Thus we note that the dynamics of the isotropic density, longitudinal, and transverse moments and other higher order spherical harmonic coefficients are coupled to each other. At this point we make an approximation and consider the coupling only to the leading order spherical harmonics, that is the isotropic density and the longitudinal and transverse components of the moments and neglect the coupling to the higher order coefficients. The bulk water dynamic remains the same as discussed in case 1 and is given by eq 12.

To uncouple the boundary condition, we can rewrite eq 25 in the following way,

$$\nabla_z \mathbf{A} = \mathbf{M}\mathbf{A} \tag{26}$$

where $\mathbf{M}$ is a 4×4 matrix and $\mathbf{A}$ is a 4-dimensional vector. To uncouple the equation for the different components of $\mathbf{A}$, we need to diagonalize $\mathbf{M}$ and write the components in terms of the eigenvectors of $\mathbf{M}$.

To do the following exercise, let us first choose the orientation of the bound water, Ω_b. As an example, let us consider that the bound water is oriented along the z direction that is, $\theta = 0$ and $\phi = 0$. For this case the boundary condition for a_{00}^f and a_{10}^f are coupled to each other, where as that for a_{11}^f and a_{1-1}^f are uncoupled and given by

$$\nabla_z a_{11}^f(z,q,s) = 0$$
$$\nabla_z a_{1-1}^f(z,q,s) = 0 \tag{27}$$

The above equation along with 12 leads to the following solution for a_{11}^f and a_{1-1}^f,[21]

$$a_{11/-1}^f(z,q,s) = \frac{1}{D}\int_0^\infty dz'\; a_{11/-1}^f(z',q,t=0)\; G_T^{11/-1}(z,z',q,s) \tag{28}$$

where Green's function $G_T^{11/-1}(z,z',q,s)$ is given by

$$G_T^{11/-1}(z,z',q,s) = \frac{L}{2}e^{-|z-z'|/L} + \frac{L}{2}e^{-|z+z'|/L} \tag{29}$$

where $L^2 = D/(2D_R + Dq^2 + s)$. Thus we find that the dynamics of a_{11}^f and a_{1-1}^f have only the fast time scale.

As mentioned earlier, the boundary condition for a_{00} and a_{10} still remains coupled. After expressing a_{00}^f and a_{10}^f in terms of the eigenvectors the boundary condition for the a_{00}^f component reduces to

$$\nabla_z a_{00}^f(z,q,s) = \frac{\alpha}{\pi}a_{00}^f(z,q,s) + \frac{\sqrt{3}\alpha}{4\pi}a_{10}^f(z=0,q,s) - \frac{3\alpha}{4\pi}a_{00}^f(z=0,q,s) - \frac{k_2'}{D(s+k_2)}\frac{1}{\sqrt{4\pi}}\rho_b(q,\Omega,t=0) \tag{30}$$

and that of the a_{10}^f component reduces to

$$\nabla_z a_{10}^f(z,q,s) = \frac{\alpha}{\pi}a_{10}^f(z,q,s) - \frac{\alpha}{4\pi}a_{10}^f(z=0,q,s) + \frac{\sqrt{3}\alpha}{\pi}a_{00}^f(z=0,q,s) - \frac{k_2'}{D(s+k_2)}\sqrt{\frac{3}{4\pi}}\rho_b(q,\Omega,t=0) \tag{31}$$

The dynamics of the a_{00}^f and a_{10}^f are now given by

$$a_{00}^f(z,q,s) = \frac{1}{D}\int_0^\infty dz'\; a_{00}^f(z',q,t=0)\; G_T^{00}(z,z',q,s) + \left[\frac{3\alpha}{4\pi}a_{00}^f(z=0,q,s) - \frac{\sqrt{3}\alpha}{4\pi}a_{10}^f(z=0,q,s) + \frac{k_2'}{D(s+k_2)}\frac{1}{\sqrt{4\pi}}\rho_b(z,q,\Omega_b,t=0)\right]G_T^{00}(z,z'=0,q,s) \tag{32}$$

and

$$a_{10}^f(z,q,s) = \frac{1}{D}\int_0^\infty dz'\; a_{10}^f(z',q,t=0)\; G_T^{10}(z,z',q,s) + \left[\frac{\alpha}{4\pi}a_{10}^f(z=0,q,s) - \frac{\sqrt{3}\alpha}{\pi}a_{00}^f(z=0,q,s) + \frac{k_2'}{D(s+k_2)}\sqrt{\frac{3}{4\pi}}\rho_b(z,q,\Omega_b,t=0)\right]G_T^{10}(z,z'=0,q,s) \tag{33}$$

where Green's functions for a_{00}^f and a_{10}^f are G_T^{00} and G_T^{10}, respectively, and given by

$$G_T^{00}(z,z',q,s) = \frac{L_0}{2}e^{-|z-z'|/L_0} + \frac{L_0}{2}e^{-|z+z'|/L_0}\left(\frac{1-\frac{\alpha}{\pi}L_0}{1+\frac{\alpha}{\pi}L_0}\right) \tag{34}$$

$$G_T^{10}(z,z',q,s) = \frac{L}{2}e^{-|z-z'|/L} + \frac{L}{2}e^{-|z+z'|/L}\left(\frac{1-\frac{\alpha}{\pi}L}{1+\frac{\alpha}{\pi}L}\right) \tag{35}$$

where $L_0^2 = D/(Dq^2 + s)$.

We note that the dynamics at larger z is coupled to the dynamics at $z = 0$ and the dynamics at $z = 0$ of isotropic density part and the longitudinal dipole moment are still coupled to each other. We consider that at time $t = 0$ the density of the free water is homogeneous and isotropic at all z, which means that $a_{00}^f(z,q,t=0)$ and $a_{10}^f(z,q,t=0)$ are zero. We further consider that at time $t = 0$ there is a bound water oriented along the z direction, $\rho_b(z,q,\Omega_b,t=0) = 1$. This leads to the following solution of $a_{10}^f(z=0,q,s)$ in the surface layer ($z = 0$),

$$a_{10}^f(z=0,q,s) = \frac{k_2'}{D(s+k_2)}\sqrt{\frac{3}{4\pi}}\frac{L}{1+\frac{3\alpha L}{4\pi}+\frac{\alpha L_0}{4\pi}} \tag{36}$$

References and Notes

(1) Pal, S. K.; Peon, J.; Bagchi, B.; Zewail, A. H. *J. Phys. Chem. B* **2002**, *106*, 12376.
(2) Denisov, V. P.; Halle, B. *Faraday Discuss.* **1996**, *103*, 227.
(3) Otting, G.; Liepinsh, E.; Wuthrich, K. *Science* **1991**, *254*, 974.
(4) Grant, E. H.; Sheppard, R. J.; South, G. P. In *Dielectric Behavior of Biological Molecules in Solution*; Clarendon: Oxford, U.K., 1978.
(5) Bizzari, A. R.; Cannistaro, S. *J. Phys. Chem. B* **2002**, *106*, 6617.
(6) Gu, W. Schoenborn, B. P. *Proteins: Struct. Funct. Genet.* **1995**, *22*, 20.
(7) Pal, S. K.; Peon, J.; Zewail, A. H. *Proc. Natl. Acad. Sci. U.S.A.* **2002**, *99*, 1763.
(8) Peon, J.; Pal S. K.; Zewail, A. H. *Proc. Natl. Acad. Sci. U.S.A.* **2002**, *99*, 10964.
(9) Pal, S. K.; Peon, J.; Zewail, A. H. *Proc. Natl. Sci. U.S.A.* **2002**, *99*, 15297.
(10) Nandi, N.; Bagchi, B. *J. Phys. Chem. B* **1997**, *101*, 10954.
(11) Pollack, G. L.; Enyeart, J. J. *Phys. Rev. A* **1985**, *31*, 980.
(12) Bhattacharyya, S.; Bagchi, B. *J. Chem. Phys.* **1998**, *109*, 7885.
(13) Koenig, S. H. *J. Biophys.* **1995**, *69*, 593. Koenig, S. H.; Brown R. D.; Ugolini, R. *Magn. Reson. Med.* **1993**, *29*, 77.
(14) Stillinger, F. H. *Science* **1980**, *209*, 451.

(15) Laidler, K. J. *Chemical Kinetics*; Harper Row: New York, 1987.
(16) Nienhuys, H. K.; Santen, R. A. V.; Bakker, H. J. *J. Chem. Phys.* **2000**, *112*, 8487.
(17) Ohmine, I.; Tanaka H.; Wolynes, P. G. *J. Chem. Phys.* **1988**, *89*, 5852.
(18) Sciortino, F.; Geiger, A.; Stanley, H. E. *J. Chem. Phys.* **1992**, *96*, 3857.
(19) Roy, S.; Bagchi, B. *J. Chem. Phys.* **1993**, *99*, 9938. Nienhuys, H. K.; Saten, R. A. V.; Bakker, H. J. *J. Chem. Phys.* **2000**, *112*, 8487.
(20) Price, W. S.; Ide, H.; Arata, Y. *J. Phys. Chem. A* **1999**, *103*, 448.
(21) Wallace, P. R. *Mathematical Analysis of Physical Problems*; Dover Publications: New York, 1984.
(22) Zwanzig, R. *Nonequilibrium Statistical Mechanics*: Oxford University Press: New York, 2001.
(23) Bagchi, B.; Biswas, R. *Adv. Chem. Phys.* **1999**, *109*, 207.
(24) In the previous theory,[1] a Fourier transform was taken along the z axis and the wavenumber was chosen such that it corresponds to solute−solvent diameter σ_{12}. To compare our results with the earlier theory, we have also performed the integration along the z axis from $z = 0$ to $z = \sigma_{12}$.
(25) Rips, I.; Klafter, J.; Jortner, J. *J. Chem. Phys.* **1988**, *89*, 4288.
(26) Chandra, A. *Phys. Rev. Lett.* **2000**, *85*, 768.
(27) Onsager, L.; Fuoss, R. M. *J. Chem. Phys.*, **1932**, **36**, 2689.